

# Towards quantitative prediction of proteasomal digestion patterns of proteins

Denis S Goldobin<sup>1,2</sup> and Alexey Zaikin<sup>3,4</sup>

<sup>1</sup> Department of Physics and Astronomy, University of Potsdam, Postfach 601553,

D-14415 Potsdam, Germany

<sup>2</sup> Department of Theoretical Physics, Perm State University, 15 Bukireva Street, 614990 Perm, Russia

<sup>3</sup> Department of Mathematical and Biological Sciences, University of Essex, Wivenhoe Park, CO4 3SQ Colchester, UK

<sup>4</sup> Departments of Mathematics and Institute for Women's Health, University College London, Gower Street, WC1E 6BT London, UK  
E-mail: [Denis.Goldobin@gmail.com](mailto:Denis.Goldobin@gmail.com) and [Zaikin.Alexey@gmail.com](mailto:Zaikin.Alexey@gmail.com)

Received 12 June 2008

Accepted 7 July 2008

Published 5 January 2009

Online at [stacks.iop.org/JSTAT/2009/P01009](http://stacks.iop.org/JSTAT/2009/P01009)

doi:10.1088/1742-5468/2009/01/P01009

**Abstract.** We discuss the problem of proteasomal degradation of proteins. Though proteasomes are important for all aspects of cellular metabolism, some details of the physical mechanism of the process remain unknown. We introduce a stochastic model of the proteasomal degradation of proteins, which accounts for the protein translocation and the topology of the positioning of cleavage centers of a proteasome from first principles. For this model we develop a mathematical description based on a master equation and techniques for reconstruction of the cleavage specificity inherent to proteins and the proteasomal translocation rates, which are a property of the proteasome species, from mass spectroscopy data on digestion patterns. With these properties determined, one can quantitatively predict digestion patterns for new experimental set-ups. Additionally we design an experimental set-up for a synthetic polypeptide with a periodic sequence of amino acids, which enables especially reliable determination of translocation rates.

**Keywords:** molecular networks (theory), regulatory networks (theory), protein function and design (theory)

---

**Contents**

<b>1. Physical model of the system and mathematical description</b>	<b>3</b>
<b>2. Short (25–50 AA) synthetic polypeptides</b>	<b>6</b>
<b>3. Long synthetic polypeptides of a periodic amino acid sequence</b>	<b>9</b>
<b>4. Long natural proteins</b>	<b>11</b>
<b>5. Conclusion</b>	<b>13</b>
<b>Acknowledgments</b>	<b>14</b>
<b>References</b>	<b>14</b>

---

A macromolecular complex, the proteasome, is the complex molecular machine for the degradation of intracellular proteins [1]. In particular, proteasomes produce epitopes for an immune system [2]. They exist in cells as the free proteolytically active core, the barrel-shaped 20S proteasome (figure 1), and as associations of this core with regulatory complexes PA700 (19S regulator) or PA28 (11S regulator) at its ends [3]. This paper deals with proteasomal digestion of proteins widely studied in molecular biology and immunology.

A protein enters the proteasome and is transported into the central chamber (this process is referred to as the *translocation* one) where it is cleaved into fragments by one of the cleavage terminals arranged along two rings. Fragments of the protein produced are removed through proteasome gates. Some of these fragments, epitopes, are transported onto the cell surface where T-lymphocytes scan them in order to recognize the cells to be killed because of an abnormal functioning. Hence, the digestion pattern for a degraded protein and its statistical properties determine the reaction of the immune system to the presence of this protein in a certain cell. Peculiarities of the translocation rates can qualitatively affect the expression of the specific fragment, e.g., an epitope, because an altered transport changes time of being near the cleavage terminal, i.e., conditions of cleavage. Moreover, impairment of proteasomal degradation, probably due to transport malfunction, might contribute to the pathology of various neurodegenerative conditions [4].

The mechanism of protein translocation remains unknown (however, subjects related to some extent to this problem have been studied in [5]–[8]). It is also unknown whether this mechanism is qualitatively different for different proteasome types (constitutive or immuno-type), with/without different regulatory complexes. Recently, in [9] a stochastic model, which allows a straightforward reconstruction of the translocation rates and cleavage specificities from mass spectroscopy (MS) data on digestion patterns, has been introduced. These properties reconstructed can be used for a comprehensive quantitative prediction of proteasomal digestion patterns for new proteins and new experimental set-ups. In this paper we elaborate the mathematical theories for the employing of the introduced model for relatively *short synthetic polypeptides* (section 2), *long proteins with*

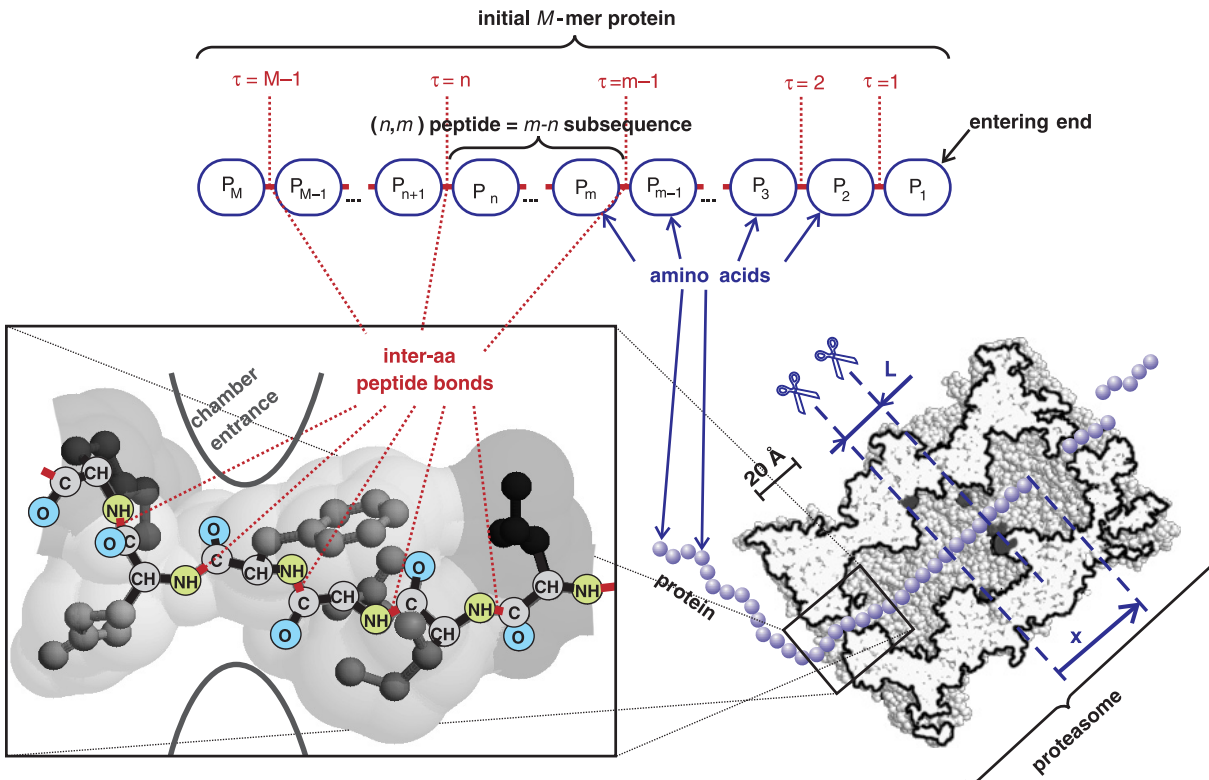


**Figure 1.** Infiltration of a protein strand into the 20S proteasome: the scissors mark the positions of active sites rings at  $x = 0$  and  $L$ ; the cleavage occurs via the attaching–detaching of the protein to active sites (dark gray color). The zoom-in shows the protein fragment KEFNII passing through the gate; the electron shields are presented in pale colors.

a periodic sequence of amino acids (section 3), and long natural proteins which require a peculiar approach (section 4).

## 1. Physical model of the system and mathematical description

We describe the process of protein transport and degradation by the proteasome (see figure 1) within the framework of the following assumptions.

- *Protein translocation.* The process of the infiltration of a protein into the proteasome chamber is a sequence of thermal noise induced jumps of the protein strand by one amino acid (AA). In figure 1, the zoom-in of the chamber gate schematically shows the diameter of the gate to be comparable with the characteristic size of an AA, which means that the protein chain may be fixed in metastable states by a tight gate between successive jumps due to large thermal fluctuations. Indeed, the atomic force measurements reveals  $U_b/kT > 3$  [10], where  $U_b$  is the characteristic height of the energy barrier separating nearest metastable positions of the chain and  $kT/2$  is the energy of thermal fluctuations. The probability of the protein shift by one AA during the infinitesimal time interval  $dt$  into the proteasome (to the right in figure 1)

is assumed to depend only on the length  $x$  of the protein forward end beyond the active sites nearest to the proteasome chamber gate used for protein infiltration (the left ones in figure 1); this probability divided by  $dt$  is given by the translocation rate function (TRF)  $v(x) \equiv v_x$ . In such a way, we neglect the role of the AA sequence specificity for translocation, what is suggested by a non-covalent interaction between the proteasome and the retracted protein. The backward motions of the entering strand are neglected as well (from [10], for the potential energy  $U(x)$  of the metastable state  $x$ ,  $(U(x-1) - U(x+1))/2kT \approx 2.5$ , thus, meaning the probability of a backward motion to be diminished by factor  $e^{-2.5}$  against the forward one). These assumptions do not impose significant restrictions on the physical mechanism of the translocation process: they are valid for the thermal drift in a tilted spatially periodic potential (e.g., see [11]) as well as for the ratchet effect (e.g., see [8]), etc. The TRFs of different proteasome species (20S, 26S which is the association of 20S core and 19S regulatory complexes, etc [3]) differ.

- *Cleavage.* When the protein strand is close to the active site, the probability of cleavage during the infinitesimal time interval  $dt$  depends on the sequence of AAs nearest to the peptide bond cleaved [12]. For the given protein, this conditional probability divided by  $dt$ , in other words, conditional cleavage rate (CCR),  $\gamma(\tau) \equiv \gamma_\tau$ , is a function of the bond number  $\tau$  (precisely,  $\tau$  enumerates the position of the bond within the initial protein and is counted from the end which has first entered the proteasome; see figure 1). In the following we use the number  $\tau$  of the bond nearest to the first ring of active sites as a *time-like variable*.
- *Removal of digestion products.* The cleaved parts of the protein degraded, peptides, leave the chamber through the second proteasome gate. Due to their mobility being higher in comparison to that of the protein, processed peptides leave the chamber quickly enough for us to neglect both their possible further splitting and their influence on the protein translocation.

Let us now introduce the distribution  $w(x|\tau)$  which is the probability of the protein forward end beyond the first ring of the active sites being of the length  $x$ , when the  $\tau$ th bond is near that ring, in terms we use henceforth, at the discrete ‘time moment’  $\tau$ . We measure  $x$  in AA. Note,  $x$  and  $\tau$  are integer. In the following we describe the ‘temporal’ evolution of distribution  $w(x|\tau)$ . In this way, we treat the shift of the protein strand into the proteasome for one AA, i.e., the transition  $\tau \rightarrow \tau + 1$ . Let us decompose  $w(x|\tau + 1)$  as

$$w(x|\tau + 1) = \sum_j w_j(x|\tau + 1),$$

where  $w_j(x|\tau + 1)$  are the contributions due to different scenarios of this transition. Along with  $w(x|\tau)$ , we account for  $Q(n, m|\tau)$ , the amount of the peptide  $(n, m)$ , which is the  $m$ - $n$  subsequence of the degraded protein (see figure 1), generated during transition  $\tau \rightarrow \tau + 1$ .

In the process of protein digestion there are three possible elementary events:

- the strand shift:  $x \rightarrow x + 1$ ,  $\tau \rightarrow \tau + 1$ ; the event rate is  $v(x)$ ;
- the cleavage on the first ring of cleavage centers ( $x = 0$ ):  $x \rightarrow 0$ ,  $\tau \rightarrow \tau$ ; the event rate is  $\gamma(\tau)$ ;
- the cleavage on the second ring of cleavage centers ( $x = L$ ,  $L$  is the distance between the rings of cleavage centers):  $x \rightarrow L$ ,  $\tau \rightarrow \tau$ ; the event rate is  $\gamma(\tau - L)$ .

In terms of these elementary events the possible scenarios of transition  $\tau \rightarrow \tau + 1$  are:

(1) Elementary event (a). Its probability is

$$P_1(x|\tau) = \begin{cases} v_x/(v_x + \gamma_\tau), & x \leq L; \\ v_x/(v_x + \gamma_\tau + \gamma_{\tau-L}), & x > L. \end{cases}$$

In this scenario,  $x \rightarrow x + 1$ , and

$$w_1(x + 1|\tau + 1) = P_1(x|\tau) w(x|\tau). \quad (1)$$

No peptides are generated.

(2) Elementary event (b), which may not be followed by anything but the strand shift by one AA (as there is nothing to be cleaved). This scenario probability is

$$P_2(x|\tau) = \begin{cases} \gamma_\tau/(v_x + \gamma_\tau), & x \leq L; \\ \gamma_\tau/(v_x + \gamma_\tau + \gamma_{\tau-L}), & x > L. \end{cases}$$

In this scenario,  $x \rightarrow 1$ , and

$$w_2(x|\tau + 1) = \delta_{x,1} \sum_{x'=1}^{\infty} P_2(x'|\tau) w(x'|\tau). \quad (2)$$

The peptides cut out are

$$Q_2(\tau, \tau - x + 1|\tau) = P_2(x|\tau) w(x|\tau). \quad (3)$$

(3) Elementary event (c), which may be followed either by strand shift (1) or by scenario (2). The probability of the first stage (c) is

$$P_c(x|\tau) = \begin{cases} 0, & x \leq L; \\ \gamma_{\tau-L}/(v_x + \gamma_\tau + \gamma_{\tau-L}), & x > L. \end{cases}$$

After event (c), when  $x \rightarrow L$ , the number of the system states generated is

$$w_c(x|\tau) = \delta_{x,L} \sum_{x'=L+1}^{\infty} P_c(x'|\tau) w(x'|\tau),$$

and the peptides cut out are

$$Q_c(\tau - L, \tau - x + 1|\tau) = P_c(x|\tau) w(x|\tau).$$

The subsequent events (1) or (2) should be considered as the respective above mentioned scenarios starting with the distribution  $w_c(x|\tau)$ , i.e.,

$$w_{c1}(x|\tau + 1) = P_1(L|\tau) w_c(x - 1|\tau) = P_1(L|\tau) \delta_{x,L+1} \sum_{x'=L+1}^{\infty} P_c(x'|\tau) w(x'|\tau), \quad (4)$$

$$Q_{c1}(\tau - L, \tau - x + 1|\tau) = P_1(L|\tau) Q_c(\tau - L, \tau - x + 1|\tau) = P_1(L|\tau) P_c(x|\tau) w(x|\tau); \quad (5)$$

$$w_{c2}(x|\tau + 1) = \delta_{x,1} \sum_{x'=1}^{\infty} P_2(x'|\tau) w_c(x'|\tau) = \delta_{x,1} P_2(L|\tau) \sum_{x'=L+1}^{\infty} P_c(x'|\tau) w(x'|\tau), \quad (6)$$

$$Q_{c2}(\tau - L, \tau - x + 1|\tau) = P_2(L|\tau) Q_c(\tau - L, \tau - x + 1|\tau) = P_2(L|\tau) P_c(x|\tau) w(x|\tau), \quad (7)$$

$$Q_{c2}(\tau, \tau - x + 1|\tau) = P_2(x|\tau) w_c(x|\tau) = \delta_{x,L} P_2(L|\tau) \sum_{x'=L+1}^{\infty} P_c(x'|\tau) w(x'|\tau). \quad (8)$$

Collecting equations (1), (2), (4), (6), one finds the *master equation*

$$w(1|\tau + 1) = \sum_{x=1}^L \frac{\gamma_\tau w(x|\tau)}{v_x + \gamma_\tau} + \left(1 + \frac{\gamma_{\tau-L}}{v_L + \gamma_\tau}\right) \sum_{x=L+1}^{\infty} \frac{\gamma_\tau w(x|\tau)}{v_x + \gamma_\tau + \gamma_{\tau-L}}; \quad (9)$$

$$w(L+1|\tau + 1) = \frac{v_L}{v_L + \gamma_\tau} \left[ w(L|\tau) + \sum_{x=L+1}^{\infty} \frac{\gamma_{\tau-L} w(x|\tau)}{v_x + \gamma_\tau + \gamma_{\tau-L}} \right]; \quad (10)$$

$$w(x|\tau + 1) = \frac{v_{x-1} w(x-1|\tau)}{v_{x-1} + \gamma_\tau + \Theta(x-L-1)\gamma_{\tau-L}} \quad \text{for } x \neq 1, \quad x \neq L+1. \quad (11)$$

Here  $x = 1, 2, 3, \dots, M$  and  $\tau = 1, 2, 3, \dots, M-1$ , where  $M$  is the length of the protein, and the Heaviside function  $\Theta(x < 0) = 0$ ,  $\Theta(x \geq 0) = 1$ . Equations (9)–(11) form a linear map

$$w(x|\tau + 1) = \sum_{y=1}^{\infty} \mathcal{L}_{xy}(\tau) w(y|\tau). \quad (12)$$

The whole contribution to the cleavage pattern is

$$\begin{aligned} Q(\tau, \tau - x + 1|\tau) &= Q_2(\tau, \tau - x + 1|\tau) + Q_{c2}(\tau, \tau - x + 1|\tau) \\ &= \frac{\gamma_\tau w(x|\tau)}{v_x + \gamma_\tau + \Theta(x-L-1)\gamma_{\tau-L}} + \frac{\delta_{x,L} \gamma_\tau}{v_L + \gamma_\tau} \sum_{x'=L+1}^M \frac{\gamma_{\tau-L} w(x'|\tau)}{v_{x'} + \gamma_\tau + \gamma_{\tau-L}}; \end{aligned} \quad (13)$$

$$\begin{aligned} Q(\tau - L, \tau - L - x + 1|\tau) &= Q_{c1}(\tau - L, \tau - L - x + 1|\tau) + Q_{c2}(\tau - L, \tau - L - x + 1|\tau) \\ &= \frac{\gamma_{\tau-L} w(L+x|\tau)}{v_{L+x} + \gamma_\tau + \gamma_{\tau-L}}. \end{aligned} \quad (14)$$

All the rest (not specified by expressions (13), (14)) of the elements  $Q(m, n|\tau)$  are zero. The expressions for digestion pattern  $Q(m, n)$  after the processing of a single protein molecule are different for short polypeptides and long ones of a periodic AA sequence.

## 2. Short (25–50 AA) synthetic polypeptides

First we consider degradation of *short* (25–50 AA) *synthetic polypeptide* (protein), the most common situation for *in vitro* experiments. Here we start at  $\tau = 1$  with  $w(x|\tau = 1) = \delta_{x,1}$  and iterate linear map (12) to the last  $\tau = M - 1$ . For a short polypeptide the releasing of the last fragment from the chamber at the ‘time moment’  $\tau = M$  should be additionally taken into account:  $Q(M, M - x + 1|M) \rightarrow Q(M, M - x + 1|M) + w(x|M)$ . Hence, with  $w(x|\tau)$  known for  $\tau = 1, 2, \dots, M$ , one may evaluate digestion pattern  $Q(m, n)$  from (13) and (14),

$$\begin{aligned} Q(\tau_1, \tau_2) &= Q(\tau_1, \tau_2|\tau_1) + \Theta(M - \tau_1 - L) Q(\tau_1, \tau_2|\tau_1 + L) \\ &= \delta_{\tau_1, M} w(\tau_1 + L - \tau_2 + 1|M) + \frac{\gamma_{\tau_1} w(\tau_1 - \tau_2 + 1|\tau_1)}{v_{\tau_1 - \tau_2 + 1} + \gamma_{\tau_1} + \Theta(\tau_1 - \tau_2 - L)\gamma_{\tau_1 - L}} \end{aligned}$$



$$\begin{aligned}
& + \frac{\delta_{\tau_1 - \tau_2 + 1, L} \gamma_{\tau_1}}{v_L + \gamma_{\tau_1}} \sum_{x=L+1}^M \frac{\gamma_{\tau_1 - L} w(x|\tau_1)}{v_x + \gamma_{\tau_1} + \gamma_{\tau_1 - L}} \\
& + \Theta(M - \tau_1 - L) \frac{\gamma_{\tau_1} w(\tau_1 + L - \tau_2 + 1|\tau_1 + L)}{v_{\tau_1 + L - \tau_2 + 1} + \gamma_{\tau_1 + L} + \gamma_{\tau_1}}, \tag{15}
\end{aligned}$$

where  $1 \leq \tau_2 \leq \tau_1 \leq M$ . Since the protein may be cleaved starting both from the C terminal and from the N terminal, the final digestion pattern is given by

$$Q_{\text{fin}}(\tau_1, \tau_2) = P_N Q_N(\tau_1, \tau_2) + P_C Q_C(M - \tau_2 + 1, M - \tau_1 + 1). \tag{16}$$

The subscripts indicate which terminal goes first;  $P_N$  and  $P_C = 1 - P_N$  are the probabilities of the degradation starting from the corresponding end. Generally,  $v_N(x)$  and  $v_C(x)$  may be slightly different, but here we neglect this difference. Note that a fragment length distribution  $S(x)$  (often used in the literature [13]) is then the convolution

$$S(x) = \sum_{\tau=x}^M Q(\tau, \tau - x + 1). \tag{17}$$

Digestion pattern  $Q_{\text{fin}}(\tau_1, \tau_2)$  is a functional of TRF  $v(x)$  and CCR  $\gamma(\tau)$ . Utilizing MS data on the digestion pattern, one can determine non-zero values of  $\gamma(\tau)$  (i.e. positions of possible cleavage) and minimize the mismatch between  $Q_{\text{fin}}(\tau_1, \tau_2)$  and MS data  $\tilde{Q}(\tau_1, \tau_2)$  over  $v(x)$ , the non-zero values of  $\gamma(\tau)$ , and  $P_N$  in order to *reconstruct* them. Expecting the function  $v(x)$  to be smooth, we parameterize appropriate approximate functions as

$$v_{\text{app}}(x) = v_0 e^{-(A_2^2/\sqrt{A_1^2+x}) + (A_2^2/|A_1|) - A_3^2(\sqrt{A_1^2+x} - |A_1|)}. \tag{18}$$

Note that  $v(x)$  and  $\gamma(\tau)$  are defined up to a constant multiplier, which should be determined from the degradation rate in real time, but not from the digestion pattern.

In order to verify the robustness of the reconstruction procedure, numerous tests have been performed. A typical test presented in figure 2 has been performed in four steps.

(1) For given  $v(x)$  (not generic for  $v_{\text{app}}$ , i.e., the function  $v(x)$  used cannot be perfectly fitted with expression (18)) and  $\gamma(\tau)$ , digestion pattern  $Q(\tau_1, \tau_2)$  has been evaluated.

(2) The result has been perturbed by the noise,  $\tilde{Q}_{\tau_1 \tau_2} = Q_{\tau_1 \tau_2} + 10^{-4} R_{\tau_1, \tau_2} \sqrt{Q_{\tau_1, \tau_2}}$ , where  $R_{\tau_1, \tau_2}$  are independent random numbers uniformly distributed in  $[-1, 1]$ .

(3) We have omitted the information about fragments, whose relative amount is less than  $5 \times 10^{-3}$ , and 1mer and 2mer fragments as being hardly detectable in experiments (one cannot distinguish identical AAs cut out from different parts of the polypeptide [16]).

(4) The resulting  $\tilde{Q}_{\tau_1 \tau_2}$  has been used for the reconstruction of  $v(x)$  and  $\gamma(\tau)$ .

The original and reconstructed data for  $\gamma(\tau)$  (figure 2(a)) and  $v(x)$  (figure 2(b)) are in a very good agreement. The reconstructed value is  $P_N = 0.52$  against original  $P_N = 0.50$ .

Unfortunately, the data available in the literature are mainly too incomplete (a lot of fragments are not accounted for) and not precise enough for a truly reliable reconstruction [9] (the initial solutions used for experiments quite frequently contain not only the polypeptide to be digested but also a certain amount of its fragments, the first measurement of the proportions of the solution is performed too late, when considerably more than 5% of the initial substrate has been degraded and one may not neglect re-entries of the digestion fragments into the proteasome, etc).

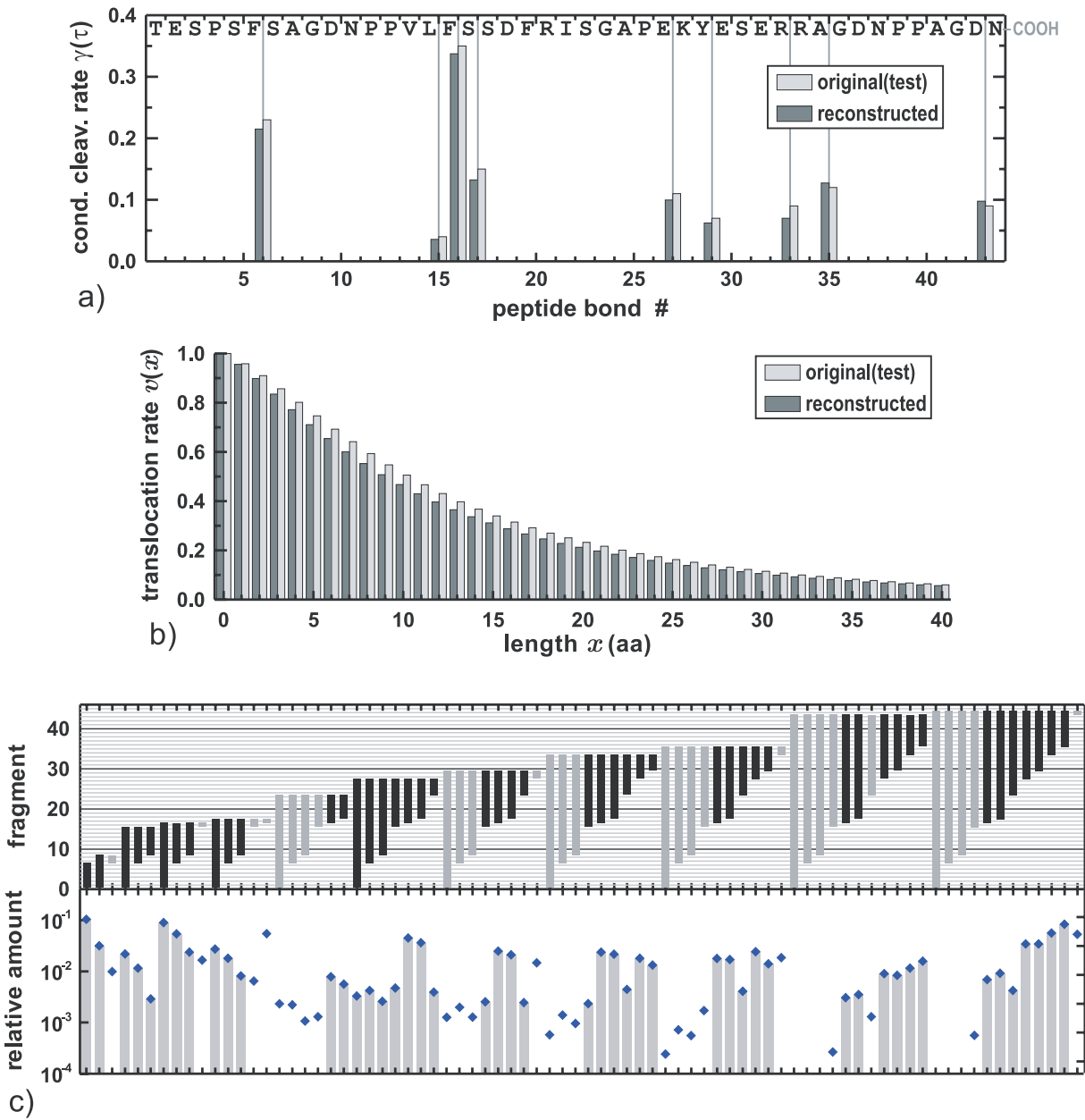


**Figure 2.** Test—reconstruction of translocation rate function  $v(x)$  and conditional cleavage rates  $\gamma(\tau)$  for the 44mer peptide Kloe 316 [14, 15] (but with roughly estimated authentic (original) values of  $\gamma(\tau)$ ), which is the subsequence 543–586 AA of human myelin associated glycoprotein. (a) The conditional cleavage rates and the AA sequence; (b) the translocation rate function; (c) the upper plot presents the set of digestion fragments (black bars: fragments utilized for the reconstruction; gray bars: not utilized), and the lower plot presents the amount of the corresponding fragment (diamonds: the reconstructed values  $Q_{\text{fin}}$ ; gray bars: the values of  $\tilde{Q}$  utilized for the reconstruction).



Thus, we should note the limitations of the suggested reconstruction method:

- The reconstruction procedure for short polypeptides is very sensitive to measurement inaccuracy.
- For some polypeptides the procedure fails. This may happen due to a specific arrangement of cleavage positions, when for different TRFs  $v(x)$  provides almost identical digestion patterns.
- Though complete information on  $Q(\tau_1, \tau_2)$  is not needed, the number of non-zero values of  $Q(\tau_1, \tau_2)$  required for a reliable (tolerant to noise) reconstruction is at least twice the number of reconstructed parameters, i.e.  $2 \times ([\text{number of positions of potential cleavage}] + [\text{number of parameters of } v_{\text{app}}] + 1)$ . For instance, for Kloe 258 in [9] the number of trustworthy and utilized values of  $\tilde{Q}(\tau_1, \tau_2)$  is 19 instead of the required  $2 \times (10 + 3 + 1) = 28$ ; it is a bit greater than the number of unknown parameters, i.e., 14. Hence, more accurate and comprehensive MS data on the digestion pattern are required.
- For short polypeptides the finishing stage of the degradation is relatively important, while in this stage the translocation rate is affected by the edge effects (the backward end of the polypeptide gets inside the proteasome chamber) and is not the same as for the remainder of the polypeptide.

### 3. Long synthetic polypeptides of a periodic amino acid sequence

While a more comprehensive acquisition of data on digestion fragments and enhancement of experimental techniques for short polypeptides are left to experimentalists, we propose an experimental set-up which allows overcoming all the limitations mentioned above and is expected to be realizable. For this a *long synthetic polypeptide with a  $T$ -periodic AA sequence*:  $\gamma(\tau) = \gamma(\tau + T)$  should be digested. Here ‘long’ means that one may neglect the peculiarities of the starting and finishing stages of the degradation, and  $M \gg T$ .

For the given direction of the degradation, e.g., starting with the N terminal, we are looking for the establishing of a solution  $T$ -periodic in  $\tau$ ,  $w_{N,T}(x|\tau) = w_{N,T}(x|\tau - T)$ , to equation (12). The fragment  $(n, m)$  is identical to the  $(n + kT, m + kT)$  one, where  $k$  is integer; therefore  $Q_N(m, n)$  may be chosen to make a contribution to  $Q_N(m - n + (n \bmod T), n \bmod T)$ . The amount of fragments grows almost linearly with ‘time’  $\tau$  as the polypeptide is being processed. Hence, for the digestion pattern one finds

$$\begin{aligned}
 Q_{N,T}(\tau_1, \tau_2) &\equiv \lim_{\tau \rightarrow \infty} \frac{1}{\tau} \sum_{\tau'=1}^{\tau} Q_N(\tau_1, \tau_2|\tau') = \frac{1}{T} \sum_{\tau'=1}^T Q_{N,T}(\tau_1, \tau_2|\tau') \\
 &= \frac{1}{T} \left[ \frac{\gamma_{\tau_1} w_{N,T}(\tau_1 - \tau_2 + 1|\tau_1)}{v_{\tau_1 - \tau_2 + 1} + \gamma_{\tau_1} + \Theta(\tau_1 - \tau_2 - L)\gamma_{\tau_1 - L}} \right. \\
 &\quad \left. + \frac{\delta_{\tau_1 - \tau_2 + 1, L} \gamma_{\tau_1}}{v_L + \gamma_{\tau_1}} \sum_{x=L+1}^{\infty} \frac{\gamma_{\tau_1 - L} w_{N,T}(x|\tau_1)}{v_x + \gamma_{\tau_1} + \gamma_{\tau_1 - L}} + \frac{\gamma_{\tau_1} w_{N,T}(\tau_1 + L - \tau_2 + 1|\tau_1 + L)}{v_{\tau_1 + L - \tau_2 + 1} + \gamma_{\tau_1 + L} + \gamma_{\tau_1}} \right]
 \end{aligned} \tag{19}$$

(here  $1 \leq \tau_2 \leq T$  and  $\tau_1 \geq \tau_2$ ).

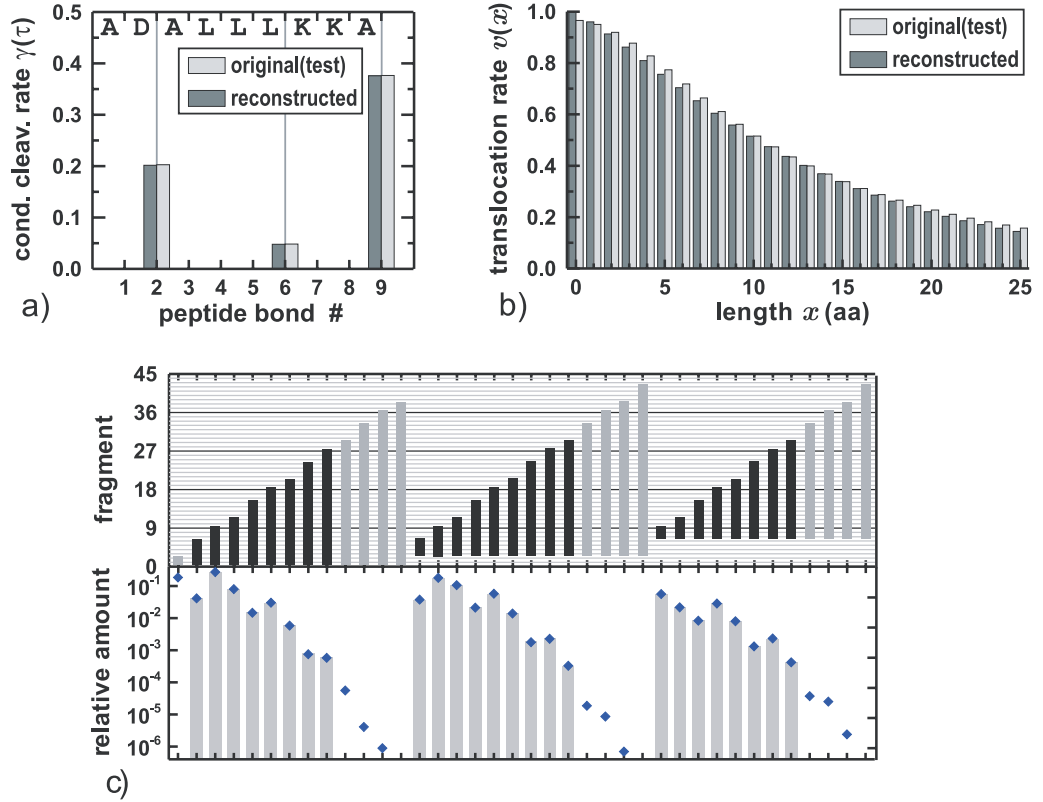


**Figure 3.** Test—reconstruction of translocation rate function  $v(x)$  and conditional cleavage rates  $\gamma(\tau)$  for a 9-periodic polypeptide with the cleavage positions 2, 6, 9. (For description see the caption to figure 2.)

To treat the degradation process starting with the C terminal, one has (i) to perform the transformation  $\gamma(\tau) \rightarrow \gamma(T - \tau)$ , (ii) to iterate linear map (12) with the new  $\gamma(\tau)$  like for the N case, but assuming  $Q_C(m, n|\tau)$  to make a contribution to  $Q_C(m \bmod T, n - m + (m \bmod T))$ . Unlike for (16), the final result is

$$Q_{\text{fin}}(\tau_1, \tau_2) = P_N Q_{N,T}(\tau_1, \tau_2) + P_C Q_{C,T}(T - \tau_2, T - \tau_1).$$

Matching  $Q_{\text{fin}}(m, n)$  to the MS data one can reconstruct  $v(\tau)$ ,  $\gamma(\tau)$ , and  $P_N$ . For a test we have made use of the cleavage map of the digestion of yeast enolise-1 by human erythrocyte proteasome [17]. Looking at its subsequence 331–348 AA,



(vertical stripes mark the positions of experimentally observed cleavages), one may expect the case where the underlined subsequence is followed not by KV, but by KKA..., and the periodic sequence is



to be realizable. For such a sequence a test like the one in figure 2 (but with much stronger dithering:  $\tilde{Q}_{\tau_1 \tau_2} = Q_{\tau_1 \tau_2} + 2 \times 10^{-3} R_{\tau_1, \tau_2} \sqrt{Q_{\tau_1, \tau_2}}$ ) is presented in figure 3. Due to the small number of unknown parameters the reconstruction procedure is rather tolerant to

measurement inaccuracy and does not require information on a large number of digestion fragments (the most easily detectable fragments are enough).

#### 4. Long natural proteins

The case of most immediate interest is the digestion of long natural proteins (over about 300 AA) because it concerns the *in vivo* proteasomal activity. A direct implementation of the procedure developed for short polypeptides is hardly possible here, as in the course of matching  $Q(\tau_1, \tau_2)$  to the MS data, one has to perform a minimization over an enormous number of parameters. However, for long non-periodic proteins, one may assume  $\gamma(\tau)$  to be a random process in order to evaluate some observable statistical properties like the fragment length distribution (FLD) of the digestion products, i.e.  $S(x)$  (see equation (17)).

For this random process we adopt the following:

- the neighbor values  $\gamma(\tau)$  and  $\gamma(\tau + 1)$  are mutually independent (which does not necessarily mean that CCR  $\gamma(\tau)$  is independent of neighbor AAs);
- $\gamma(\tau)$  is zero with a certain probability  $q$ , and has a finite probability density  $g(\gamma)$  otherwise.

The normalized mean FLD  $\mathcal{S}(x) \equiv \langle S(x) \rangle / \sum_{x'=1}^{\infty} \langle S(x') \rangle$  may be evaluated either via the plain iteration of (12)–(16) with noise  $\gamma(\tau)$  over a large interval of  $\tau$  or via the direct simulation of the system with a Gillespie algorithm (e.g., see [18]). However, the calculation procedure may be considerably facilitated. For this purpose, let us average (12) over realizations of  $\gamma(\tau)$ ,

$$\langle w(x|\tau + 1) \rangle_{\gamma} = \sum_{y=1}^{\infty} \langle \mathcal{L}_{xy}(\tau) w(y|\tau) \rangle_{\gamma}. \quad (20)$$

Notably,  $w(x|\tau)$  depends on  $\gamma(\tau - 1)$  and the preceding values of  $\gamma$  but is independent of  $\gamma(\tau)$ . Moreover, the impact of preceding values of  $\gamma$  decays in the course of the processing of the protein, and one may neglect the correlation between  $w(x|\tau)$  and  $\gamma(\tau - L)$  which are mutually distant in  $\tau$ . Thus,  $w(x|\tau)$  is independent of  $\gamma(\tau)$  and  $\gamma(\tau - L)$ , which are involved in  $\mathcal{L}_{xy}(\tau)$ , and (20) yields

$$\langle w(x|\tau + 1) \rangle_{\gamma} \approx \sum_{y=1}^{\infty} \langle \mathcal{L}_{xy}(\tau) \rangle_{\gamma\tau\gamma\tau-L} \langle w(y|\tau) \rangle_{\gamma}; \quad (21)$$

from (13), (14), (17),

$$\begin{aligned} \langle S(x|\tau + 1) \rangle_{\gamma} &= \langle S(x|\tau) \rangle_{\gamma} + \left\langle \frac{\gamma_{\tau}}{v_x + \gamma_{\tau} + \Theta(x - L - 1)\gamma_{\tau-L}} \right\rangle_{\gamma\tau\gamma\tau-L} \langle w(x|\tau) \rangle_{\gamma} \\ &+ \left\langle \frac{\gamma_{\tau-L}}{v_{L+x} + \gamma_{\tau} + \gamma_{\tau-L}} \right\rangle_{\gamma\tau\gamma\tau-L} \langle w(L + x|\tau) \rangle_{\gamma} \\ &+ \delta_{x,L} \sum_{x'=L+1}^{\infty} \left\langle \frac{\gamma_{\tau}}{v_L + \gamma_{\tau}} \cdot \frac{\gamma_{\tau-L}}{v_{x'} + \gamma_{\tau} + \gamma_{\tau-L}} \right\rangle_{\gamma\tau\gamma\tau-L} \langle w(x'|\tau) \rangle_{\gamma}, \end{aligned} \quad (22)$$

where

$$\begin{aligned} \langle f(\gamma_1, \gamma_2) \rangle_{\gamma_1 \gamma_2} &\equiv q^2 f(0, 0) + q(1 - q) \int_0^\infty g(\gamma) [f(0, \gamma) + f(\gamma, 0)] d\gamma \\ &+ (1 - q)^2 \int_0^\infty d\gamma_1 \int_0^\infty d\gamma_2 g(\gamma_1) g(\gamma_2) f(\gamma_1, \gamma_2). \end{aligned}$$

The FLD observed in experiments is  $\mathcal{S}(x)$ , corresponding to the establishing of the steady solution  $\langle w(x|\infty) \rangle$  to linear map (21).

Notably, with the additional approximation

$$\langle \mathcal{L}_{xy}(\gamma_\tau, \gamma_{\tau-L}) \rangle_{\gamma_\tau \gamma_{\tau-L}} \approx \mathcal{L}_{xy}(\langle \gamma \rangle, \langle \gamma \rangle),$$

one may obtain an implicit recursive formula for establishing  $\langle w(x|\tau) \rangle$  from (21),

$$\langle w(x+1|\infty) \rangle = \frac{(1 + \delta_{x,L}) v_x}{v_x + (1 + \Theta(x-L)) \langle \gamma \rangle} \langle w(x|\infty) \rangle, \quad (23)$$

and find FLD  $\mathcal{S}(x)$  from (22),

$$\begin{aligned} \mathcal{S}(x) &= \\ &\frac{((1 + \delta_{x,L}) \langle \gamma \rangle \langle w(x|\infty) \rangle) / (v_x + (1 + \Theta(x-L)) \langle \gamma \rangle) + (\langle \gamma \rangle \langle w(L+x|\infty) \rangle) / (v_{L+x} + 2 \langle \gamma \rangle)}{\langle w(1|\infty) \rangle + (\langle w(L+1|\infty) \rangle) / 2}. \end{aligned} \quad (24)$$

Remarkably, in the quasi-continuous limit (which is valid when  $v(x)$  is a ‘slow’ function of  $x$ ), the last expressions provide (cf [18])

$$\begin{aligned} \langle w(x|\infty) \rangle &= (1 + \Theta(x-L)) \langle w(0|\infty) \rangle \exp\left(-\int_0^x \frac{(1 + \Theta(x-L)) \langle \gamma \rangle}{v(x')} dx'\right), \\ \mathcal{S}(x) &= \langle \gamma \rangle \frac{\frac{\exp(-\int_0^x \frac{(1 + \Theta(x-L)) \langle \gamma \rangle}{v(x')} dx')}{v(x)} + \frac{\exp(-\int_0^{L+x} \frac{(1 + \Theta(x-L)) \langle \gamma \rangle}{v(x')} dx')}{v(L+x)}}{1 + \exp(-\int_0^L \frac{\langle \gamma \rangle}{v(x')} dx')}. \end{aligned}$$

In figure 4, one may see that both above mentioned approximations become more accurate as  $q$  decreases. However, for a realistic value  $q \approx 3/4$  which is suggested by experimental cleavage maps (see figure 2, where the sites of a potential cleavage are taken from experimental data), the approximation (21) and (22) works considerably better than the (23) and (24) one. Remarkably, as  $q$  increases with  $\langle \gamma \rangle$  kept fixed, the local maximum near  $x = L$  shifts from  $x = L$  to higher values of fragment length  $x$  and the cutting out of longer peptides becomes more probable. The existence of this maximum at  $L \approx 8-10$  AA deserves especial attention because the epitopes, involved in the functioning of the immune system and bound to MHC I molecules, have exactly such length [19].

The important limitation of this method is related to the reconstruction of  $v(x)$  for 1mer and 2mer peptides. These peptides are hardly detectable in experiments and, therefore, experimental  $\mathcal{S}(x)$  is not determined for  $x = 1, 2$ , and one cannot reconstruct the respective values of  $v(x)$ . Note that for methods suggested in sections 2 and 3 this limitation does not occur because, e.g., for the subsequence |F|S|SDFRISGAPE| in figure 2, the information on  $v(1)$  is reflected in the difference between the readily measurable amounts of generated peptides |S|SDF...| and |SDF...|, while for long natural proteins we lose the individual information on each specific peptide cut out.

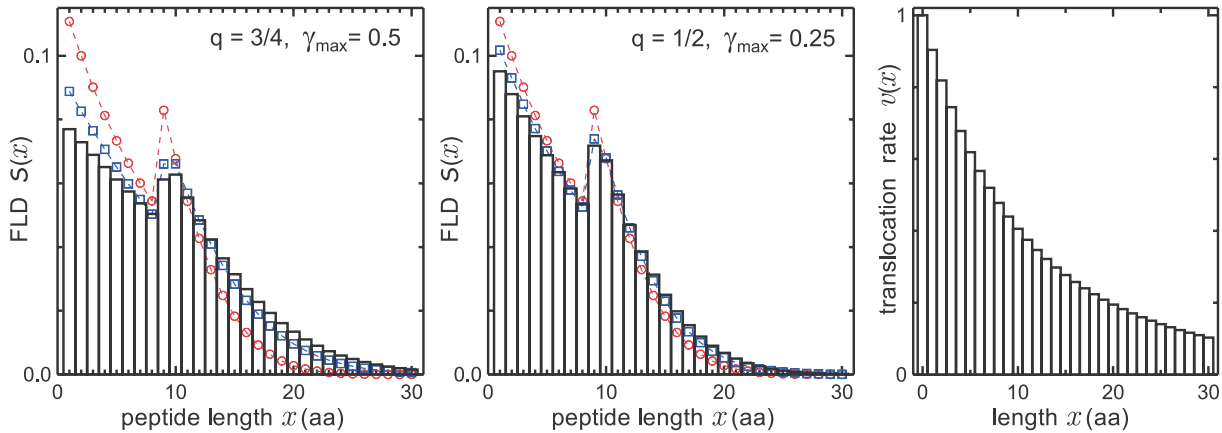


**Figure 4.** Samples of fragment length distribution  $\mathcal{S}(x)$  (FLD) for the degradation of a long natural protein under the assumption that conditional cleavage rate  $\gamma(\tau)$  may be treated as a random process. The fraction  $q$  of non-scissile peptide bonds is indicated in the plots, non-zero values of  $\gamma(\tau)$  are uniformly distributed in  $[0, \gamma_{\max}]$ ,  $L = 9$ , and the adopted translocation rate function  $v(x)$  is plotted in the right plot. In two left plots, bars: results of the direct simulation with a Gillespie algorithm, squares: the approximation (21), (22), circles: the approximation (23), (24) with  $\langle \gamma \rangle = (1 - q)\gamma_{\max}/2$ .

## 5. Conclusion

In this paper we have discussed a model of the degradation of proteins by the proteasome which allows one to *reconstruct* the proteasomal translocation function and the cleavage specificity inherent to the amino acid sequence and not affected by proteasomal transport properties. With these properties determined, one can comprehensively predict digestion patterns of new proteins. The model is relevant for a broad variety of hypothetically possible translocation mechanisms [8, 11]. We have mathematically elaborated this model for the cases of (i) relatively short (25–50mers) synthetic polypeptides as the most common case for *in vitro* experiments, (ii) long periodic polypeptides (proposed experiments with such polypeptides are very promising for reverse engineering), and (iii) long natural proteins.

In [18], we have already discussed how peculiarities of the translocation function may lead to the multimodality of the fragment length distribution even for  $\gamma(\tau) = \text{const}$ . Here we have shown that the amount of each digestion fragment is not only determined by the cleavage map (specifically, conditional cleavage rate  $\gamma(\tau)$ ) of the substrate but is also crucially affected by non-uniformity of the translocation rate. The results of implementation of the developed theory for processing experimental data on digestion patterns for different proteasome species under different conditions can give insight into the nature of the protein translocation mechanism inside the proteasome. They can also elucidate the unanswered question of whether there is some preference for starting the degradation with the N terminal or C terminal of the protein, and how this preference is affected by regulatory complexes. Hopefully, theoretical results will stimulate new experiments as suggested in this paper for the case of a periodic polypeptide.

## Acknowledgments

We are grateful to Susanne Witt and Michele Mishto for useful discussions. The work was supported by grants of the VW-Stiftung, the BRHE program, and the Foundation ‘Perm Hydrodynamics’.

## References

- [1] Rock K L, Gramm C, Rothstein L, Clark K, Stein R, Dick L, Hwang D and Goldberg A L, 1994 *Cell* **78** 761
- [2] Kloetzel P M, 2001 *Nat. Rev. Mol. Cell. Biol.* **2** 179
- [3] Tanahashi N, Murakami Y, Minami Y, Shimbara N, Hendil K B and Tanaka K, 2000 *J. Biol. Chem.* **275** 14336
- [4] Rubinsztein D C, 2006 *Nature* **443** 780  
Mishto M, Bellavista E, Santoro A and Franceschi C, 2007 *Central Nervous System Agents in Medicinal Chemistry* **7** 236
- [5] Holzhütter H G and Kloetzel P M, 2000 *Biophys. J.* **79** 1196
- [6] Peters B, Janek K, Kuckelkorn U and Holzhütter H G, 2002 *J. Mol. Biol.* **318** 847
- [7] Luciani F, Kesmir C, Mishto M, Or-Guil M and de Boer R J, 2005 *Biophys. J.* **88** 2422
- [8] Zaikin A and Pöschel T, 2005 *Europhys. Lett.* **69** 725
- [9] Goldobin D S, Mishto M, Textoris-Taube K, Kloetzel P M and Zaikin A, *Reverse engineering of proteasomal translocation rates*, 2008 *Preprint* 0804.0682 submitted
- [10] Witt S, 2007 private communication
- [11] Reimann P, Van den Broeck C, Linke H, Hänggi P, Rubi J M and Perez-Madrid A, 2001 *Phys. Rev. Lett.* **87** 010602
- [12] Tenzer S, Peters B, Bulik S, Schoor O, Lemmel C, Schatz M M, Kloetzel P M, Rammensee H G, Schild H and Holzhütter H G, 2005 *Cell. Mol. Life Sci.* **62** 1025
- [13] Kisselev A F, Akopian T N and Goldberg A L, 1998 *J. Biol. Chem.* **273** 1982
- [14] Mishto M *et al*, 2006 *Biol. Chem.* **387** 417
- [15] Mishto M, Luciani F, Holzhütter H G, Bellavista E, Santoro A, Textoris-Taube K, Franceschi C, Kloetzel P M and Zaikin A, 2008 *J. Mol. Biol.* **377** 1607
- [16] Kohler A, Cascio P, Leggett D S, Woo K M, Goldberg A L and Finley D, 2001 *Mol. Cell* **7** 1143
- [17] Nussbaum A K, Kuttler C, Haderl K-P, Rammensee H-G and Schild H, 2001 *Immunogenetics* **53** 87
- [18] Zaikin A, Mitra A K, Goldobin D S and Kurths J, 2006 *Biophys. Rev. Lett.* **1** 375
- [19] Falk K, Röttschke O, Stevanovic S, Jung G and Rammensee H G, 1991 *Nature* **351** 290  
Madden D R, Gorga J C, Strominger J L and Wiley D C, 1991 *Nature* **353** 321